Horizontally propagating three-dimensional chemo-hydrodynamic patterns in the chlorite-tetrathionate reaction

Éva Pópity-Tóth,[1] Dezső Horváth,[1] and Ágota Tóth[1, a)]

Department of Physical Chemistry and Materials Science, University of Szeged, Aradi vértanúk tere 1., Szeged, H-6720, Hungary

(Dated: 13 July 2012)

Planar reaction fronts resulting from the coupling of exothermic autocatalytic reactions and transport processes can be deformed by convection in the presence of gravity field. We have experimentally investigated how buoyancy affects the spatiotemporal pattern formation at various solution thicknesses in three-dimensional medium. In the chlorite–tetrathionate reaction a stable structure propagating horizontally with constant velocity and geometry develops when appropriately thick solutions are studied. Both the horizontal and the vertical projections of the resulting three-dimensional structures are quantitatively characterized: the smooth leading edge of the front is independent of the solution thickness and the structured trailing edge ends in a center cusp with a constant angle.

[a)]E-mail: atoth@chem.u-szeged.hu

A vertical planar reaction front in a fluid medium is always unstable hydrodynamically under gravity if the density of the reactant and the product mixture is different. The geometry of the front—defined as the thin zone where the autocatalytic reaction takes place—is distorted as the less dense fluid tends to advance on top of the other. The propagation of such a self-organized interface is investigated experimentally in a three-dimensional medium, where the density decrease results from the temperature rise caused by the exothermic reaction. Simultaneous monitoring from the top and the side reveals that the arising front has a smooth leading profile and a structured trailing edge ending in a cusp. The systematic variation of the thickness of the container indicates that for sufficiently thick medium the self-sustained front takes on a stable structure propagating at a constant velocity. The mixing length associated with the leading edge of the front is found to be independent of the thickness, giving rise to a cell with constant amplitude in the vertical projection of the front image. Within the front zone the segments of ascending product solution coalesce at a constant angle forming the center cusp, which is only stable in thicker medium, otherwise it exhibits transverse motion.

I. INTRODUCTION

The interaction of chemical reactions with transport processes may lead to various spatiotemporal patterns in distributed systems.[1] One of the simplest forms is a reaction front propagating in a homogeneous medium due to the coupling of diffusion with an autocatalytic process providing the positive feedback. The chemical front, defined as the thin zone where the reaction takes place at considerable rate, spatially separates the fresh reactants from the products.

In the gravitational field, the arising convective motion of a fluid medium represents an additional process contributing to the pattern formation.[2] Density may vary in the course of a chemical reaction because the change in composition leads to the change in the partial molar volumes of the components and/or the exo- or endothermicity of the reaction results in a temperature rise or drop. The front may therefore separate two fluids with different

density. In aqueous solutions, the hydrodynamic stability of the system depends on the orientation of the reaction front.[3,4] For a horizontal front propagating in either direction an unstable stratification occurs if the solution with greater density lies on top of the other.[5–8] The arising fluid motion will distort the reaction front leading to cellular pattern in a process also termed density fingering. Simple convection takes place when the solutal and thermal components of the density change have the same sign, i.e, they are cooperative, resulting in a monotonous variation of density.[5] In this case the opposite orientation generally represents a hydrodynamically stable system where no convection arises with the exception of a special scenario when the difference in diffusion coefficients leads to local inversion of density.[9] With opposing solutal and thermal contributions, multicomponent convection arises, in which case both orientations may lead to the Rayleigh-Taylor instability of the planar reaction front.[10–12] A vertical reaction front separating two solutions with different density is always unstable as the denser liquid tends to sink under the other, and the arising convection will distort the advancement of the reaction front.[13–15] It is important to mention that although the reactant and product mixtures are miscible, an autocatalytic reaction front maintains a constant gradient between the two solutions, therefore the system in many aspects may resemble an immiscible nonreactive case.

In thin solution layers the hydrodynamic instability of a propagating reaction front has been thoroughly investigated both experimentally[5–7,10] and theoretically[8,16–21]. Two model reactions have been the subject of studies: the iodate–arsenous acid (IAA) reaction[5], in which both the solutal and the thermal density change have a negative sign at room temperature, and the chlorite–tetrathionate (CT) reaction[6], where the two contributions are antagonist. In the latter system with conditions where thermal effects are negligible, simple convective patterns have been observed for horizontal reaction fronts propagating downwards as the products of the reaction is denser than the reactants.[6] The reaction is highly exothermic, therefore in thicker layers with insufficient heat removal to the surroundings, thermal effects[22] have led to multicomponent convection.[11] Studies of the horizontal propagation of vertical reaction fronts in thin vertical layers have resulted in the theoretical formulation[9,14,23] and experimental verification[15,24,25] of various scaling laws associated with the geometry of the evolving stable front structure governed by a single convection roll.

A more complex scenario is expected to arise in three-dimensional systems not only because the hydrodynamics involved cannot be considered as a potential flow, but also due to

the inevitable thermal component of the density change in case of exothermic reactions. For fronts propagating along the gravity field, the additional temperature gradient on the one hand may lead to the formation of thermal plumes,[10] on the other hand can stabilize fingering patterns on a longer time scale.[26] When heat effects become dominant for horizontally propagating fronts in reactions with opposite signs in the solutal and thermal components of density change, the orientation of the reaction fronts may reverse and the pattern will continuously change, as shown in the CT reaction.[27] Recently, the effect of heat has been investigated experimentally in the IAA reaction in thick channels varying the height of the solution layer.[28] A stable V-shaped pattern evolves when the height is less than 7 mm, while parabolic shaped structure develops for solutions with height greater than 13 mm. Intriguing three-dimensional convection patterns can also be observed in an isothermal system: in a thin layer with conditions set to slow down the horizontal propagation of a CT reaction front, we have found both oscillatory and stationary modes of convective patterns in the wake of the reacting interface.[29]

In this current study, we utilize the chlorite oxidation of tetrathionate in slight chlorite excess with stoichiometry according to[30,31]

$$7\mathrm{ClO_2^-} + 2\mathrm{S_4O_6^{2-}} + 6\mathrm{H_2O} = 7\mathrm{Cl^-} + 8\mathrm{SO_4^{2-}} + 12\mathrm{H^+} \tag{1}$$

to generate horizontally propagating reaction fronts in a three-dimensional medium. We systematically vary the physical size of the medium by adjusting the geometry of the reaction vessel containing the aqueous solution and quantitatively characterize the evolving convective pattern.

In this work, our aim is to describe the spatiotemporal pattern formation and to characterize experimentally the behavior of horizontally propagating vertical chemical fronts developed in three dimensions in tube. We systematically varied the parameters related to the geometry of the reaction vessels. We create experimental conditions which do not eliminate thermal effects, and described the emerging patterns.

II. EXPERIMENTAL

Throughout the experiments, reagent-grade materials (Sigma, Aldrich, Reanal) of the chlorite–tetrathionate reaction are used except for sodium chlorite (Aldrich) which is applied

in the commercially available technical grade form. The solution with composition in Table I are mixed and poured into a vertically positioned 20 cm long, 11 mm high reaction vessel with adjustable thickness L_y of 6, 11, 16, and 21 mm, constructed from four 35 mm thick flat glass walls shown in Fig. 1. Bromophenol blue indicator is selected to visualize the chemical reaction: the original basic reactant solution is blue which changes its color to purple then to yellow in the course of the reaction as the mixture turns acidic. The ratio of the reactants is set to $[NaClO_2]_0/[K_2S_4O_6]_0 = 4$ in each experiment in order to maintain a constant chlorite excess. The reaction fronts are initiated electrochemically at the anode by applying a 3 V potential difference between two thin Pt-wire electrodes (0.25 mm in diameter) positions horizontally at one end of the container. The reaction front arising initially deforms and propagates horizontally across the vessel. The evolution of this pattern is monitored at room temperature simultaneously from both the top and the side as illustrated in Fig. 2. In the experiments, we focus our attention to the stable chemical fronts in the central region of the reaction vessel, excluding the transition zone in the vicinity of the initiation. The images are recorded in 1 s intervals by a color digital camera (Sony DFW-X710) connected to a computer. In separate sets of experiments, temperature profiles across the reaction fronts are obtained by utilizing a type J thermocouple (0.5 mm in diameter) immersed in the solution at two preset depths.

The front edge of the reaction zone—the transition from blue to purple—is defined as the point of inflection in the blue color component of the recorded image along the direction of propagation (x-coordinate), from which the mean front position can be determined by averaging it along the direction perpendicular to propagation (z-coordinate). For each experiment, in which a final front geometry develops, the leading front edge is characterized by the mixing length and the temporal average of the stable front profiles. The mixing length is given experimentally as the standard deviation of the front position, while the temporal average, determined only for the time period characterized with profiles having constant mixing length and shape, is the time average of the profiles with their average front position shifted to zero. In this work, generally one hundred profiles are evaluated and averaged resulting in an error for the mixing length on the scale of the spatial resolution of the digitized images. We have repeated all experiments until the error on the reproducibility of the mixing length was less than 5 %. For each experiment the horizontal translation of the average front position along (x-direction) provides the velocity of propagation.

III. RESULTS & DISCUSSION

Under our experimental conditions, the reactant solution of the CT reaction in the vicinity of the chemical front is denser than the product. Therefore in the presence of the gravity field, the less dense products will tend to advance on top of the fresh denser reactants as seen in Figs. 3(b) and (d). The solutal component of the net density change itself is positive (3×10^{-4} g/cm^3), i.e., under isothermal conditions the product solution has greater density than the reactant. The thermal contribution, however, has opposite sign at room temperature, since the reaction is highly exothermic. This latter term dominates in the reaction vessels used in our experiments because heat can only slowly dissipate into the surrounding from the thick solution and hence the heat loss through the container wall is not efficient. Thus, the warmer product solution is less dense than the fresh reactant solution across the front[25,27]. As time progresses, the initial front becomes distorted as convection driven by the function of the overall density change sets in.

From 3 mm to 6 mm thick reaction vessels, the front profile is continuously changing. The horizontal projected images of the front in Figs. 3(b) and (d) clearly illustrate that reaction front with one or two convection rolls fitting into the 11 mm high solution has no stable geometry. By inspecting the pattern from the side in the 6 mm thick reaction vessel, we can observe a front with mixing length of 8.6±0.6 mm (approximately 1/4th of the amplitude) which has a highly asymmetric shape. Although the leading edge in the top projection (cf. Figs. 3(a) and (c)), constitutes a single symmetric cell independent of time, the trailing purple cusp—indicating a zone of ascending solution—exhibits spatial oscillation/motion transverse to the direction of propagation.

In thicker reaction vessels (with the thickness at 11 mm or above), we find that the propagating reaction front not only reaches a constant velocity of propagation but also takes on a constant shape after a short transition period. The final steady structure is asymmetric from the side as illustrated in Figs. 4(b) and (d). This horizontal view is similar to those in thinner reaction vessels (cf. Figs 3(b) and 4(b)), only the thin purple reaction zone separating the blue reactant mixture from the yellow product is now more visible. The interesting feature of this tilted reaction zone is that its leading edge, indicated by the color transition from blue to purple, forms a simple curve that resembles the geometry associated with reaction fronts propagating horizontally in a thin vertical slab; the trailing

edge, appearing as the transition from purple to yellow, however has a more structured geometry, which reveals that the local dynamics is not driven by a single large convection roll as in thin slabs. A smaller vortex dominates the top section of the reaction front, while a larger one develops towards the lower segment.

The view from the top highlights the three-dimensional structure of the tilted reaction zone (see in Fig. 4(a)). The leading edge separating the blue and purple regions forms a single symmetric cell which is most advanced in the middle corresponding to the warmer and less dense regime at the top of the solution. The bright yellow color where the reactants are essentially completely converted into the highly acidic product in the entire height of the liquid ends in a V-shaped cusp. Unlike in thinner vessels, this cusp is stationary and positioned in the center, ahead of which in the direction of the front propagation a thin blue region is visible, suggesting that the center of the three-dimensional stationary structure is characterized by an ascending warmer and less dense solution, yielding two convection rolls in Fig. 4(a).

Upon increasing the thickness of the reaction vessel to 21 mm (see Fig. 4(c)), the leading edge still forms a single cell and the single symmetric cusp in the center remains as the ending feature of the front. The reaction zone—besides appearing thicker from the side shown in Fig. 4(d)—is now characterized by two plumes of ascending solution indicated by the blue lines. Although the underlying convection pattern initially divides the thickness approximately equally into three sections, as the front propagates the blue lines associated with ascending reactant solution coalesce into the center cusp at the end, which is now a distinct feature from the side pointing backward and upward.

Since the chemical composition is constant, thermal contribution to the density change should play an important role as the thickness of the reaction vessel is increased. In thicker solutions the heat evolved dissipates more slowly to the environment as it is conducted less efficiently than in thinner reaction vessels. The enhanced thermal effects are illustrated by the temperature profiles measured at two different depths shown in Fig. 5(a) in an 11 mm thick reaction vessel. The solid line in Fig. 5(b) corresponding to the profile 0.3 mm below the top indicates a sudden increase in temperature at the leading edge of the reaction zone. The temperature then further increases at a slower rate until its highest value where all the reactants are converted into product, yielding a 2.3 °C rise overall. Beyond the reaction zone, the warmer product solution cools on a time scale significantly longer than that of our

experiment. The dashed line in Fig. 5(b) showing the temperature profile 0.7 mm below the top reveals an increase in temperature with a little delay (almost immediately after the leading edge of the reaction zone) but its initial increasing rate is smaller. The temperature peak at this depth is also reached upon the complete conversion of the reactant mixture, beyond which a similar cooling rate is observed.

In order for a quantitative description of the three-dimensional front pattern, we have characterized the distinct features of the reaction front at three different vessel thickness while keeping other experimental parameters constant. The overlap of the final leading edge in the horizontal projection presented in Fig. 6 indicates that it is independent of the thickness of the vessel and has a mixing length of 9.2±0.6 mm (approximately a quarter of the amplitude because of the definition). This is in accordance with our experimental findings in thin vertical slabs: the front profile starts as a curve on the top and ends approximately linearly at the bottom towards the back, and the entire geometry scales with the height of the container, a parameter kept constant in this study. Figure 7 depicts the vertical projection, i.e., the top view of the leading edge forming a single cell scaled with the thickness in the y-direction. In this semi-scaled presentation again the overlap of profiles shows the invariance of cell amplitude—resulted in a constant mixing length of 0.77±0.08 mm—in the direction of propagation with respect to the thickness. On the contrary, the vertical projection of the trailing cusps grows on increasing the solution thickness, and as Fig. 8 reveals the coalescing of the thin segments of ascending solution forms a constant angle independent of the thickness at the V-shaped center cusp. We also have determined the propagation velocities in all cases from both projections, and have found that it is independent of the solution thickness with value of 1.06±0.01 mm/s. Its invariance suggests that the horizontal velocity is a function of the solution height in the gravity field, similarly to thin vertical slabs.

Bou Malham et al.[24] have studied the viscous lock-exchange gravity current in the presence of the IAA reaction front and found that the ratio of front extension (L_e) and liquid height is a function of a single variable (Λ) according to

$$\left(\frac{L_e}{L_z}\right)^2 = \frac{\sqrt{1+4a^2\Lambda^2}-1}{2} \tag{2}$$

where a is a numerical factor and $\Lambda = D_{lock}/(L_z\, v_0)$ with v_0 being the velocity of the pure reaction-diffusion front which is 0.18±0.01 mm/s. The effective diffusion coefficient in the

absence of reaction (D_{lock}) involves a function of the aspect ratio (L_z/L_y) as

$$D_{lock} = \frac{L_y^2 L_z \Delta\rho\, g}{\eta} \mathcal{G}(L_z/L_y). \tag{3}$$

Unlike in our previous experiments,[25,27] the aspect ratio of the container is in the range of 0.5–1.0 for stable leading front edge, therefore the system is characterized by two-dimensional Stokes flow between distant vertical boundaries. For this case Martin et al.[32] have derived that the function $\mathcal{G}(L_z/L_y)$ is proportional to $(L_z/L_y)^2$, the substitution of which into Eq. 3 results in an effective diffusion coefficient—and hence a Λ—independent of the solution thickness L_y. This is in accordance with our findings, that is, the mixing length (a quarter of the front extension for our profiles) associated with the leading edge of the front is invariant of the thickness and only depends on the height of the liquid, which is kept constant throughout this study.

In conclusion, we have observed that the horizontal propagation of a reaction front in a sufficiently thick solution layer leads to the evolution of a three-dimensional stationary structure that has two characteristic regions: the leading symmetric edge and the V-shaped trailing cusp. The vertical projection of the leading edge forming a single cell reveals that its amplitude is independent of the solution thickness in accordance with the invariance of the horizontal projection. The latter has a geometry that characterizes fronts propagating horizontally in a thin vertical slab. The density decrease in the course of the exothermic reaction results in ascending solution segments creating a center cusp at the trailing edge of the reaction front. The cusp has a constant angle for solution thickness in the range of 11–21 mm, in which case the front velocity is also independent of the thickness, while it exhibits transverse oscillatory motion for narrower (3–6 mm thick) containers.

ACKNOWLEDGMENTS

This work was financially supported by the Hungarian Scientific Research Fund (OTKA K72365) and the European Space Agency (ESTEC 4000102255/11/NL/KML). The authors thank Eszter Tóth-Szeles for measuring the velocity of the pure reaction-diffusion front.

REFERENCES

[1]I.R. Epstein and J.A. Pojman, An Introduction to Nonlinear Dynamics: Oscillations, Waves, Patterns, and Chaos, Oxford University Press, Oxford, 1998.

[2]I. Nagypál, Gy. Bazsa and I.R. Epstein, J. Am. Chem. Soc. **108**, 3635 (1986).

[3]J. A. Pojman and I. R. Epstein, J. Phys. Chem. **94**, 4966 (1990).

[4]J. D'Hernoncourt, A. Zebib and A. De Wit, Chaos, **17**, 013109 (2007).

[5]M. Böckmann and S. C. Müller, Phys. Rev. Lett. **85**, 2506 (2000).

[6]D. Horváth, T. Bánsági, Jr., Á. Tóth, J. Chem. Phys. **117**, 4399 (2002).

[7]L. Sebestiková, J. D'Hernoncourt, M.J.B. Hauser, S.C. Müller and A. De Wit, Phys. Rev. E **75**, 026309 (2007).

[8]A. De Wit, Phys. Fluids **16**, 163 (2004).

[9]D. Lima, A. D'Onofrio and A. De Wit, J. Chem. Phys. **124**, 014509 (2006).

[10]T. Bánsági, Jr., D. Horváth, Á. Tóth, J. Yang, S. Kalliadasis and A. De Wit, Phys. Rev. E **68**, 055301 (2003).

[11]T. Bánsági, Jr., D. Horváth and Á. Tóth, Chem. Phys. Lett. **384**, 153 (2004).

[12]J. D'Hernoncourt, A. De Wit and A. Zebib, J. Fluid Mech. **576**, 445 (2007).

[13]D.A. Vazquez, J.M. Littley, J.W. Wilder and B.F. Edwards, Phys. Rev. E **50**, 280 (1994).

[14]L. Rongy, N. Goyal, E. Meiburg and A. De Wit, J. Chem. Phys. **127**, 114710 (2007).

[15]T. Tóth, D. Horváth and Á. Tóth, J. Chem. Phys. **128**, 144509 (2008).

[16]J. Huang, D. A. Vasquez, B. F. Edwards and P. Kolodner, Phys. Rev. E **48**, 4378 (1993).

[17]D. A. Vasquez, J. M. Littley, J. W. Wilder, and B. F. Edwards, Phys. Rev. E **50**, 280 (1994).

[18]D. A. Vasquez, J. W. Wilder and B. F. Edwards, J. Chem. Phys. **104**, 9926 (1996).

[19]A. De Wit, Phys. Rev. Lett. **87** 054502 (2001).

[20]J. Martin, N. Rakotomalala, D. Salin and and M. Böckmann, Phys. Rev. E **65**, 051605 (2002).

[21]S. Kalliadasis, J. Yang and A. De Wit, Phys. Fluids **16**, 1395 (2004).

[22]J. Martin, N. Rakotomalala, L. Talon and D. Salin, Phys. Rev. E **80**, 055101 (2009).

[23]N. Jarrige, I. Bou Malham, J. Martin, N. Rakotomalala, D. Salin and L. Talon, Phys. Rev. E **81**, 066311 (2010).

[24]I. Bou Malham, N. Jarrige, J. Martin, N. Rakotomalala, L. Talon and D. Salin, J. Chem.

Phys. **133**, 244505 (2010).

[25]G. Schuszter, T. Tóth, D. Horváth and Á. Tóth, Phys. Rev. E **79**, 016216 (2009).

[26]T. Tóth, D. Horváth and Á. Tóth, Chem. Phys. Lett. **442**, 289 (2007).

[27]L. Rongy, G. Schuszter, Z. Sinkó, T. Tóth, D. Horváth, Á. Tóth, A. De Wit, Chaos **19**, 023110 (2009).

[28]L. Sebestiková and M.J.B. Hauser, Phys. Rev. E **85**, 036303 (2012).

[29]O. Miholics, T. Rica, D. Horváth and Á. Tóth, J. Chem. Phys. **135**, 204501 (2011).

[30]L. Szirovicza, I. Nagypál, E. Boga, J. Am. Chem. Soc. **111**, 2842 (1990).

[31]A. K. Horváth, J. Phys. Chem. **109**, 5124 (2005).

[32]J. Martin, N. Rakotomalala, L. Talon and D. Salin, J. Fluid Mech. **674**, 132 (2011).

TABLE I. Composition of reactant solution

$[K_2S_4O_6]$/mM	5.00
$[NaClO_2]$/mM	20.00
[NaOH]/mM	5.00
Bromophenol blue/mM	0.08

Fig. 1 Scheme of the reaction cell: (a) perspective view, (b) end view.

Fig. 2 The experimental setup.

Fig. 3 Image of a front propagating from left to right at room temperature in a reaction vessel with thickness L_y=6 mm [(a)-(b)] 30 s and [(c)-(d)] 90 s after inititation. [(a)-(c)] Top view. [(b)-(d)] Side view. The light yellow region represents the product solution and the darker blue region the reactant.

Fig. 4 Image of a front propagating from left to right with constant shape at room temperature at 100 s after inititation with $L_y = 11$ mm (a) and (b), $L_y = 21$ mm (c) and (d). [(a) and (c)] Top view. [(b) and (d)] Side view. The lighter yellow region represents the product solution and the darker blue region the reactant.

Fig. 5 Image of a front propagating from left to right with constant shape at room temperature in a reaction vessel with thickness L_y=11 mm (a). Temperature profiles with a black solid line at 0.3 mm (1) and a red dashed line at 0.7 mm (2) below the surface (b).

Fig. 6 Temporal average profile of the stable front edge viewed from the side for selected vessel thicknesses: (●) 11 mm, (♦) 16 mm, and (▲) 21 mm.

Fig. 7 Temporal average profile of the stable front edge viewed from the top for selected vessel thicknesses: (●) 11 mm, (♦) 16 mm, and (▲) 21 mm.

Fig. 8 Temporal average profile of stable center cusp viewed from the top for selected vessel thicknesses: (●) 11 mm, (♦) 16 mm, and (▲) 21 mm.

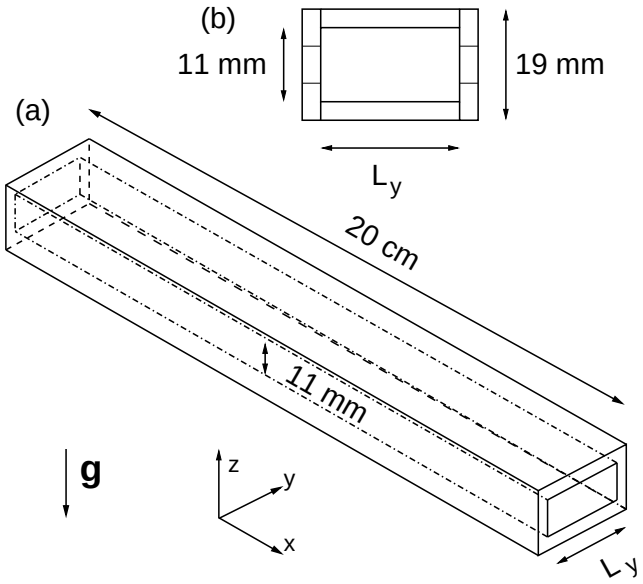

FIG. 1. É. Pópity-Tóth ... Chaos

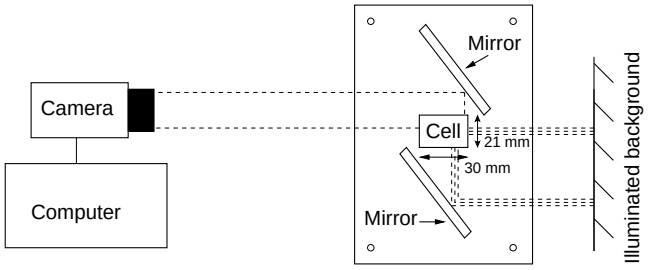

FIG. 2. É. Pópity-Tóth ... Chaos

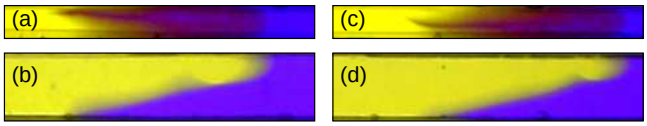

FIG. 3. É. Pópity-Tóth ... Chaos

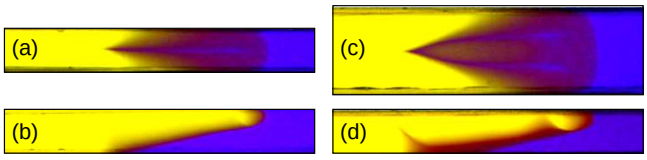

FIG. 4. É. Pópity-Tóth ... Chaos

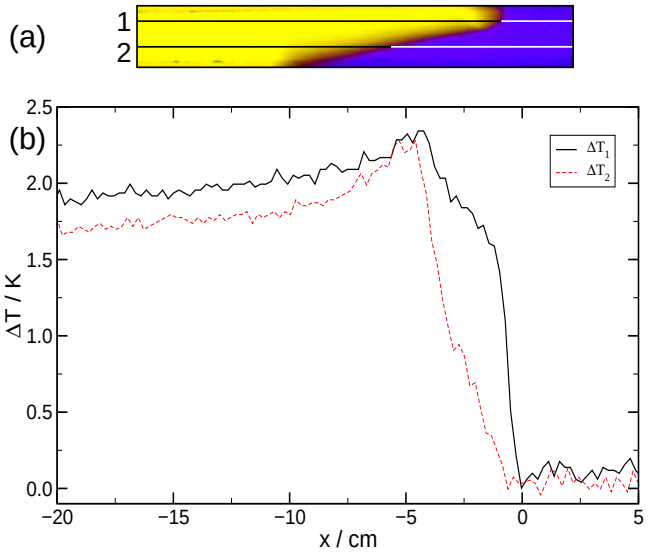

FIG. 5. É. Pópity-Tóth ... Chaos

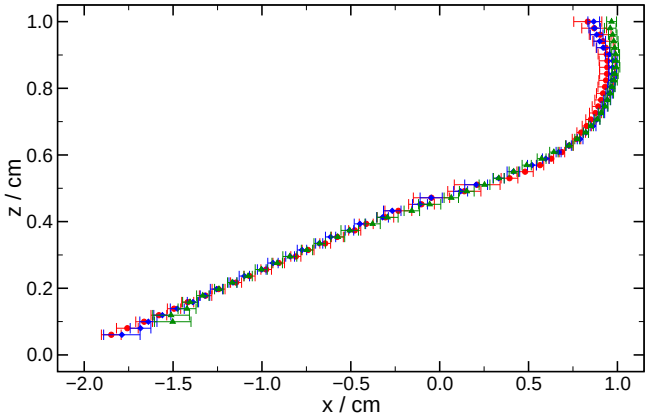

FIG. 6. É. Pópity-Tóth ... Chaos

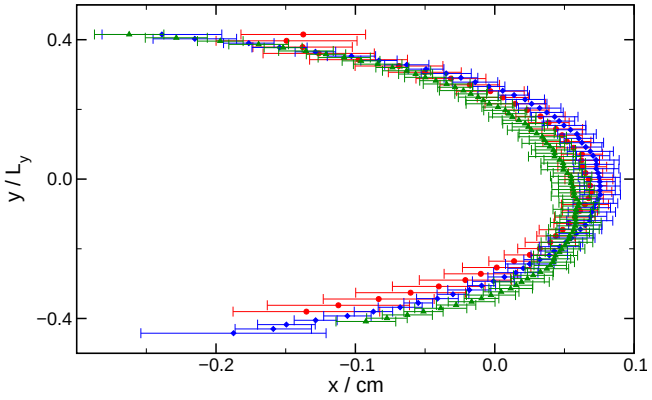

FIG. 7. É. Pópity-Tóth ... Chaos

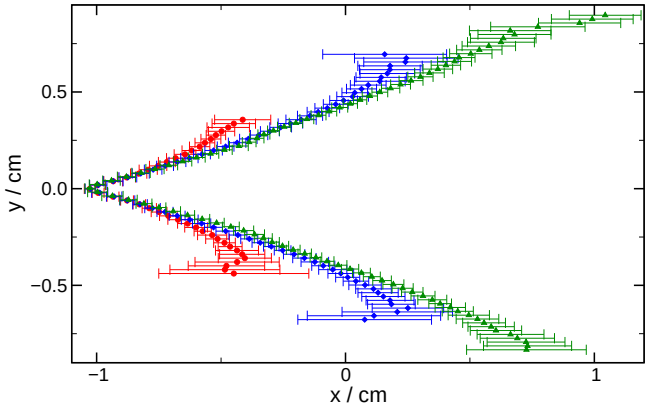

FIG. 8. É. Pópity-Tóth ... Chaos